Sub-micron Control Algorithm for Grinding and Polishing Aspherical Surface

Hyung-Tae Kim, Hae-Jeong Yang, and Sung-Chul Kim

Abstract: A position control method for interpolating aspherical grinding and polishing tool path was reviewed and experimented in a nano precision machine. The position-base algorithm was reformed from the time-base algorithm, proposed in the previous study. The characteristics of the algorithm were in the velocity control loop with position feedback. The aspherical surface was divided by an interval at which each velocity and acceleration were calculated. The theoretical velocity was corrected by position error during processing. In the experiment, a machine was constructed and nano-scale linear encoders were installed at each axis. Relation between process parameters and the variation of position error was monitored and discussed. The best result from optimized parameters showed that the accuracy was 150nm and improved from the previous report.

Keywords: Aspherical polishing, micro lenses, surface grinding, synchronized motion control, tool path generation, 2D interpolation.

1. INTRODUCTION

Aspherical lenses are widely used for current consumer electronics, industrial laser, military devices and telecommunications. The manufacturing conditions for the lenses require high accuracy and strict environment control. It is difficult to obtain the shape by conventional processing skills. According to recent articles, a few methods are reported to make the aspherical shape, by press forming [1], electro-static current [2], electrorheological fluid [3] and excimer laser micro-machining [4].

The most common method is machining such as grinding and polishing [5]. Convex or concave shaped material is fixed on the machining chuck, and the lens is shaped by removing the surface with a ceramic tool. The machining tool makes contact with the lens surface, so the tool should track along the computed position. The ideal tool path is generated from the equation of asphericity. The typical working cycle is composed of grinding, measuring and polishing. The accuracy of the grinded surface is scanned and stored in the measurement step. The amount of removal in polishing is calculated from the measurement result. CODE V is the most popular software for generating tool path and analyzing surface error [6,7]. The removal rate of the process can be determined by the size of a tool and feed rate [8]. Most of the curvature interpolation algorithms are derived from differentiation of a surface function. But aspherical equation is non-linear and complex, so it is hard to derive an interpolation algorithm from the typical method.

The authors have been developing an interpolation algorithm for tracking the aspherical tool path [9,10]. The concept of the algorithm is similar to that of discrete control. The surface is partitioned by a time interval. The movement of X axis was assumed to be driven by a constant feed rate and the velocity of Z axis was varied. Velocity and acceleration at each interval are calculated from the surface function and the properties of the previous step. Because it is difficult to control time interval on a PC, the equations on the time domain was converted to position-base ones. The ideal velocity in the process is corrected by position error. The test machine had nanoscale resolution and feedback devices. Two axes of the machine were controlled for the aspherical interpolation. The process parameters were changed to watch the effect to error variation. The response by the calibrated parameters was discussed. From the test

Manuscript received April 21, 2007; revised January 10, 2008; accepted February 21, 2008. Recommended by Editorial Board member Dong Hwan Kim under the direction of Editor Jae Weon Choi. The authors would like to thank AM Technology (http://www.amtechnology.co.kr) for supplying experimental equipments and comsumables.

Hyung-Tae Kim is with Mechatronics Team, Korea Institute of Industrial Technology, 35-3 Hongcheon, Ipjang Cheonan, Chungnam 330-825, Korea (e-mail: htkim@kitech.re.kr).

Hae-Jeong Yang is with the Dept of Mechanical Design Engineering, Korea Poly-technique University, 2121, Jeongwang, Siheung, Kyunggi, Korea (e-mail: yhj@kpu.ac.kr).

Sung-Chul Kim is with Research Center, AM Technology, 604BL-4LT, Banwol Industrial Complex, 643-3, Sungkog, Danwon, Ansan, Kyunggi, Korea (e-mail: amt@amtechnology.co.kr).

result, the proposed algorithm is simple but has enough performance to produce aspherical lens.

2. ASPHERICITY AND TOOL PATH

2.1. Equation of asphericity

An aspherical surface is all the geometric surfaces except spherical one. There are several types of aspherics, and the most common form is the conic surface of revolution plus polynominal aspheric [11]. The general form describing such aspherics is written as (1). The surface can be parabolic, hyperbolic, elliptic by changing constants in the equation. The equation of (x, z) describes the displacement from optical axis and the height of the origin [12]. The shape of the vertex is symmetrical and the origin is in zero.

$$z = f(x) = \frac{x^2}{R\left\{1+\sqrt{1-\frac{(\kappa+1)x^2}{R^2}}\right\}} + \sum_{j=1}^{20} A_j |x|^j, \quad (1)$$

where R represents the radius of curvature of the underlying shape, κ, the conic constant determines the nature of the basic deviation from sphericity, and coefficients A_j govern the magnitude of any higher deviation from the sphericity [13]. Fig. 1 shows convex and concave aspherical surfaces tested in this paper and generated by Table 1.

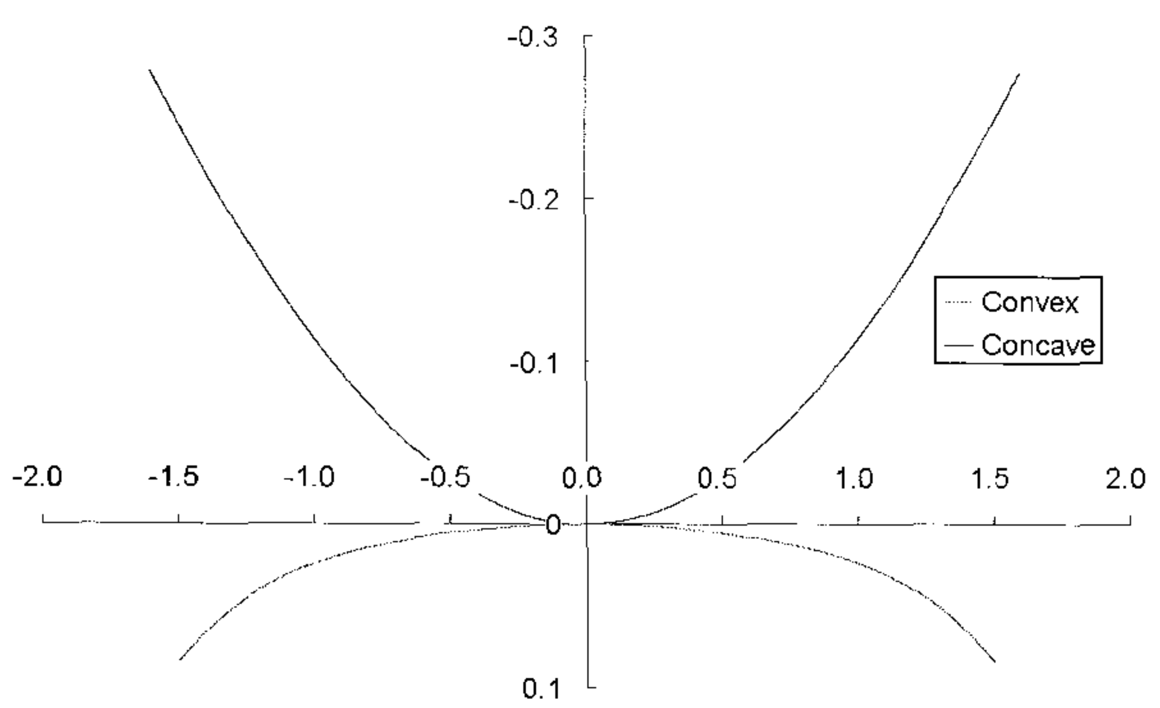

Fig. 1. Example for aspherical surfaces.

Table 1. Specifications of test machine.

	contents	specification
compoenets	controller linear encoder motor	Ajin-extek Heidenhain Mitsubishi
x axis	motor resolution gear ratio ball screw pitch feedback accuracy	20000ps/rev 1/100 4mm/rev 10nm
z axis	motor resolution gear ratio ball screw pitch feedback accuracy	20000ps/rev 1/100 4mm/rev 10nm

2.2. Tool path for aspherical surface

Common tools for grinding or polishing have spherical cylindrical shape. Points on the circumference of the tool contact with the aspherical surface. But machining position is calculated on the center of the tool, so the tool path is not coincided with the lens surface. The position of tool center can calculated from the contact point and geometric relations. The displacement between the center and the contact point can be calculated easily if the contact angle is obtained. The contact angle is derived from a tangential line on the aspherical surface. Fig. 2 shows the concept of tool contact. The tangential angle θ can be calculated from the differentiation of the equation of asphericity.

$$\tan\theta = z' = f'(x) \quad (2)$$

Procedure of differentiation for (2) is complex, so g is defined to make the procedure simpler.

$$g(x) = \sqrt{1-\frac{(\kappa+1)x^2}{R^2}} \quad (3)$$

If (3) is inserted to (1) instead of the square terms, the θ can be derived from (2) as follows [9].

$$\tan\theta = z' = \frac{2x(1+g)/R-(\kappa+1)x^3/R^3}{g(1+g)^2} + \sum_{j=1}^{20} \mathrm{sgn}(x) j A_j |x|^{j-1} \quad (4)$$

The distance between the contact point and the spherical tool can be obtained from the triangular relation shown in Fig. 2. Therefore, the position of the tool, which means the tool path, can be written as

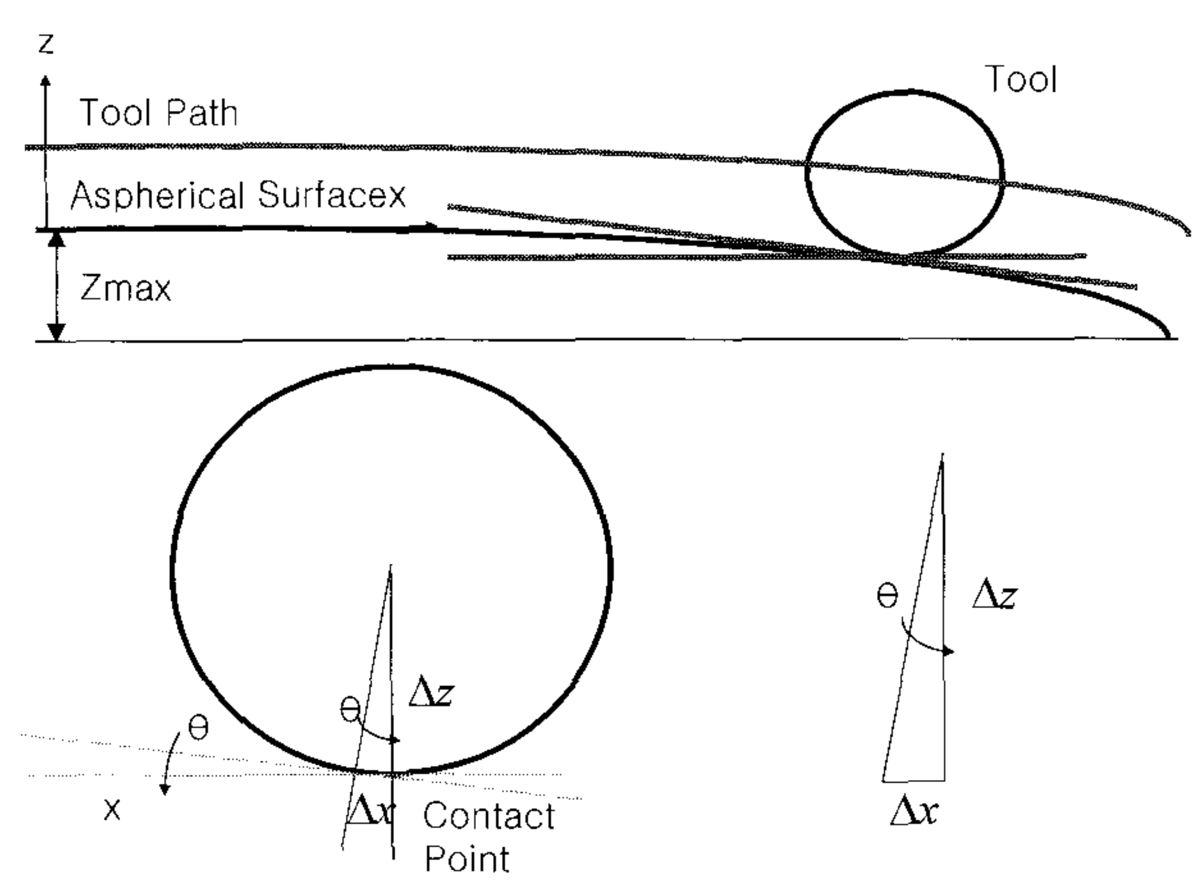

Fig. 2. Tool contaction and contact angle.

equation (5) and (6), where D_t means the tool diameter.

$$x_t = x + \Delta x = x + \frac{D_t}{2}\sin\theta \quad (5)$$

$$z_t = z + \Delta z = z - \frac{D_t}{2}\cos\theta \quad (6)$$

Because the (x_t, z_t) has a dependant variables z and θ, which can be substituted by x, the tool path function h can be defined as follows.

$$x_t = p(x), \quad z_t = q(x). \quad (7)$$

3. METHOD FOR TOOL PATH CONTROL

3.1. Interpolation concept

Conventional interpolation algorithms have been developed for NC base systems. The properties generated for tool path are position and velocity. After the path was stored as a NC code, the code is downloaded to the system. Recent PC-base controllers have function registers for inputting acceleration and deceleration as a part of motion profile. The variables can be altered even during moving on real-time, which is called override. In the previous report, authors proposed a method for generating acceleration as follows [9].

Let's assume that x moves by constant feed rate v_f, z moves by variable velocity v. The aspherical tool path will be shaped according to v_f and v. The profile is sampled at each time interval t_s as shown in Fig. 3. Each section has accelerating and constant moving. If the arbitrary acceleration connects between velocity variation of the intervals, the shape will be smoother than the acceleration is not considered. The time of accelerating t_a is a part of the divided section, and smoothness γ is defined as the ratio of accelerating time over the sampling time as shown in Fig. 4. Then, the accelerating time can be written as follows in (8).

$$t_a = t_t\gamma \quad (8)$$

Total movement in i-th step, d_i, can be written by velocity and acceleration, so it can be expressed by the following equation.

$$d_i = \frac{1}{2}a_i t_a^2 + v_i(t_s - t_a) \quad (9)$$

d_i has the same magnitude as the increment on the curve between the intervals. This relation can be expressed by (10), where $q(x_i)$ is the tool path function for the aspherical surface.

$$d_i = q(x_{i+1}) - q(x_i) \quad (10)$$

Therefore, the acceleration at i-th is derived from (9) and (10).

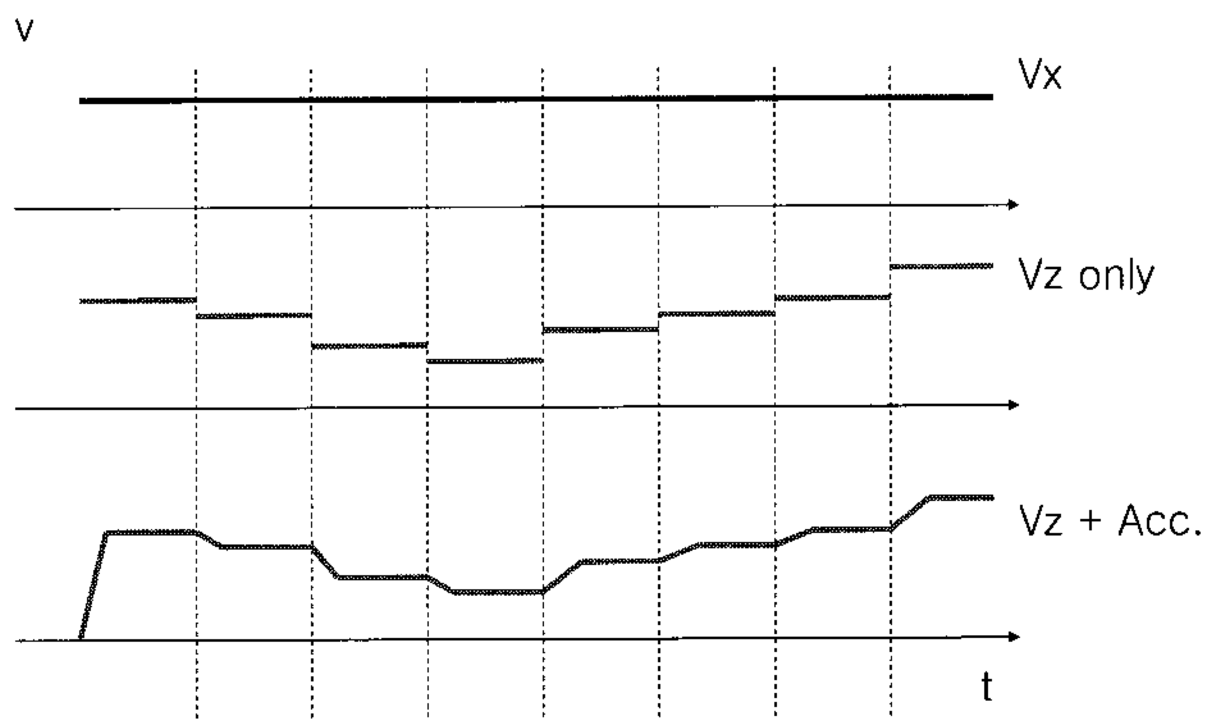

Fig. 3. Concept of smoothness due to acceleration.

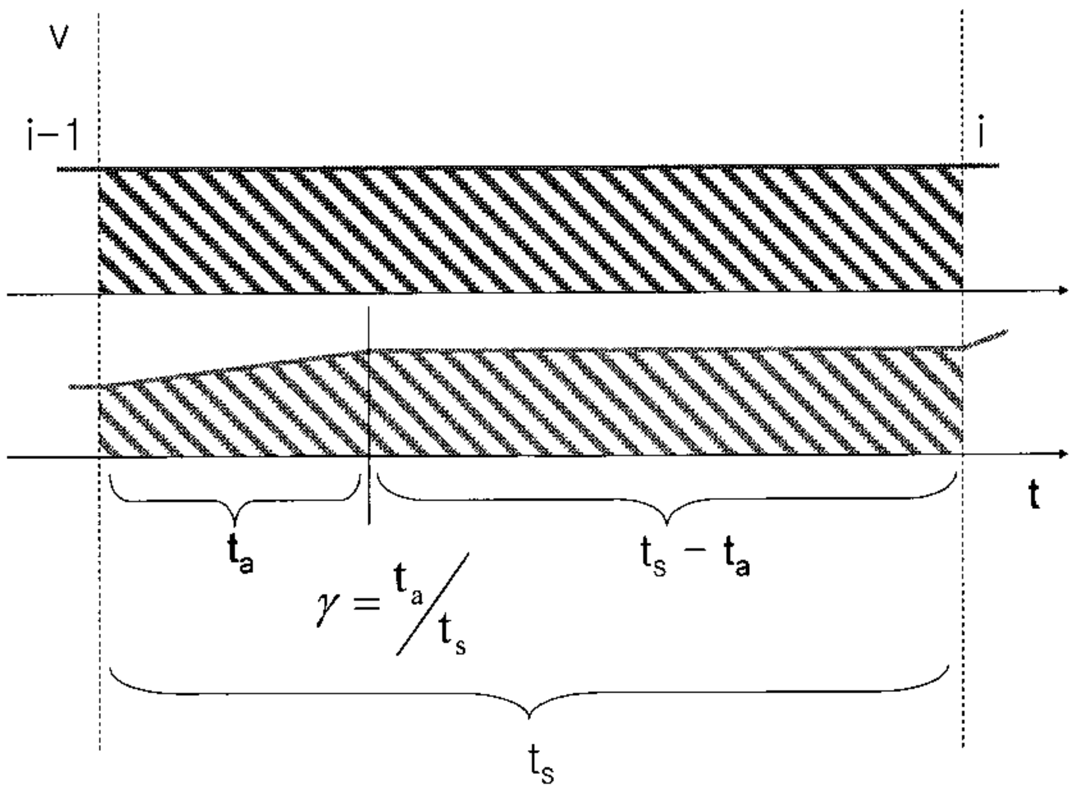

Fig. 4. Acceleration and velocity as an interval.

$$a_i = 2\frac{q(x_{i+1}) - q(x_i) - v_i t_s(1-\gamma)}{t_s^2\gamma^2} \quad (11)$$

v_i is easily obtained from the variable a_i and velocity at previous step.

$$v_i = a_i t_s\gamma + v_{i-1} \quad (12)$$

a_i is unknown variable, however a_i in the (12) can be substituted by (11). The result is shown as following equation.

$$v_i = \frac{1}{2-\gamma}\left[\frac{2}{t_s}\{q(x_{i+1}) - q(x_i)\} + \gamma v_{i-1}\right] \quad (13)$$

Now, value of v_i is determined, a_i can be calculated from the (12).

$$a_i = \frac{v_i - v_{i-1}}{t_s\gamma} \quad (14)$$

3.2. Control method

The lens design factors such as R, κ and A_j are determined as a constant, so the ideal path can be calculated by the function, $z_t = q(x)$. Then, the path is divided by an interval on x domain. In principle, the curve can be partitioned on x_t domain, but the partitioning sequence is complex and requires numerical root finding step. So, this part will be reported next paper. The controller inputs such as a_i and v_i are updated at each interval. But if the system is driven by only the ideal variables, which means an open-loop, the position offset error will occur. To compensate this position error, feedback terms should be added like the (15). The form is similar to a typical model of closed control loop. Where, v_c is corrected velocity by the feedback error and sent for controller input.

$$v_c = a_i t_s \gamma + v_{i-1} + K_p E_i + K_v \frac{\Delta E_i}{\Delta t} \tag{15}$$

E_i, position error, is defined as (16), where z_o is the z-position measured by feedback devices.

$$E_i = q(x_i) - z_o \tag{16}$$

On above equations, the velocity input is affected by the position feedback. The velocity increases or decreases by the position error. The feedback term actually means error correction speed. If there is no feedback error, the velocity will have an ideal value. The velocity is updated and corrected at each interval of the tool path. The curve is interpolated on the base of velocity control, but the feedback is position error.

One of the problems in PC base control is in the difficulty to maintain the constant time interval, because PC timer is not precise and slow. This means that position and velocity may be updated at bad timing. Concept of distance interval can be an alternative for the time interval. The time interval can be substituted easily by feed rate v_f and the distance interval δ [14].

$$t_s = \frac{\delta}{v_f} \tag{17}$$

The equations from (13) to (15) can be re-written as follows.

$$v_i = \frac{1}{2-\gamma}\left[\frac{2v_f}{\delta}\{q(x_{i+1}) - q(x_i)\} + \gamma v_{i-1}\right], \tag{18}$$

$$a_i = \frac{v_f}{\gamma\delta}(v_i - v_{i-1}), \tag{19}$$

$$v_c = \frac{a_i \gamma \delta}{v_f} + v_{i-1} + K_p E_i + K_v \frac{E_i - E_{i-1}}{h}. \tag{20}$$

4. EXPERIMENT

4.1. Control system

The machine in the test had two axes on planar direction, to which *x-z* is corresponded above theory. The aspherical tool path was interpolated by simultaneous movement of each axis. The axes were composed of linear guides and ball screws. Gear was attached between the motor and the ball screw because of increasing position resolution. Each motor was driven by a PC-base controller. Nano resolution linear encoder was installed on each axis to check position error. Table 1 show the specification of the test machine. Two air-spindles were installed in the system. One was for rotating a tool, the other for lens. The revolution of tool and lens makes the surface axis-symmetrical. The rotation speed was about 30,000rpm, so grinding friction was ignored. Fig. 5 is the photo of the machine in the experiment. The window-base operating program was implemented with VC++. The software managed design parameter, process parameter, control variables and position feedback with user-friendly interface.

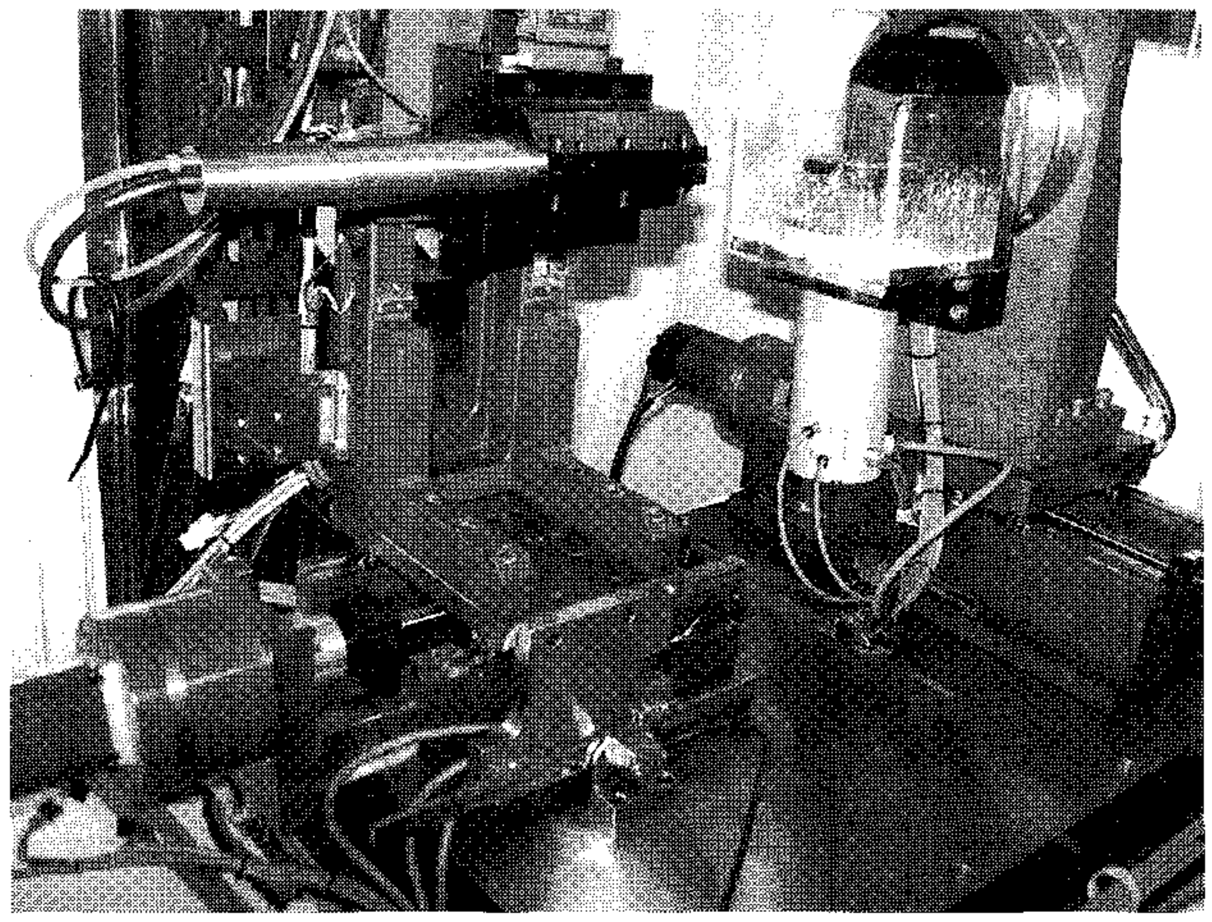

Fig. 5. Photograph of a two-axis machine for the experiment.

4.2. Procedure

The aspherical profile was generated by the constant in Table 2. The starting point was at the center of lens and the end point at the right edge. Process parameters varied in the experiment were feed rate v_f, distance interval δ, smoothness γ, control

Table 2. Standard conditions in the experiment.

	convex	concave
radius of lens	1.6mm	1.5mm
height of lens	279.19μm	84.05μm
R	22.405	-4.254
κ	43.098	-3.359
δ	1μm	2μm
v_f	20μm/s	10μm/s
γ	0.5	0.5
K_p	0.4	0.4
K_v	0.2	0.2
D_t	4.0mm	4.0mm
Temperature	21°C	19°C
Humidity	24%	28%

constant K_p and K_v.

These parameters were tested in both of the convex and concave surfaces. After the constants were set in the program, the axes were driven by the proposed algorithm.

The physical properties such as position, velocity, and position error were stored in a file. The data were analyzed for watching the effect of process parameter via position error. After optimized parameters were determined, tracking the tool path was performed. The room temperature and humidity could not be controlled precisely, the experiment was done continuously for individual parameters. The range of temperature variation was in ±2°C and that of the humidity was in ±2.5%.

5. RESULT

The v_f was varied from 0.002 to 0.03mm/s. The position error decreased at low feed rate, as shown in Figs. 6 and 7. The error tends to increase as the x stroke reaches to the end point of processing, the circumference of a lens. Z displacement at a step increased by the movement of x axis, so the z velocity should increase, which was observed in the experiment. The response is theoretically improved on the low speed, but the response by extremely low speed became worse due to initial error. This can be related with mechanical friction and driving torque in start of process. The results of high or extremely low feed were oscillated, which means the z axis could not follow the position commanded.

The δ was varied from 1% to 50% of feed rate. The position error decreased as the control interval narrower. We can expect the error response will be improved in smaller distance interval due to profiling the continuous surface into discrete one. But the response grew worse when the interval was below 1/20 of feed rate. This can be caused by minimum processing time of controller, so the controller has the timing rage which can receive the control command. Figs. 8 and 9 are the results. The γ was varied from 0.1 to 0.9. Figs. 10 and 11 show the variation of position error. The response was not much varied from 0.1 to 0.5, but the response grew worse in the range from 0.7. So, the system cannot track the tool path if the acceleration is too low. There was a peak just after start processing, which means the system did not follow initial movement. The response became worse at the circumference of a lens. This factor affects to smoothness of a curve, so it is determined from the condition of lenses after processing.

The K_p and K_v gain were varied from 0.1 to 0.5. When the K_p increased, the position error decreased.

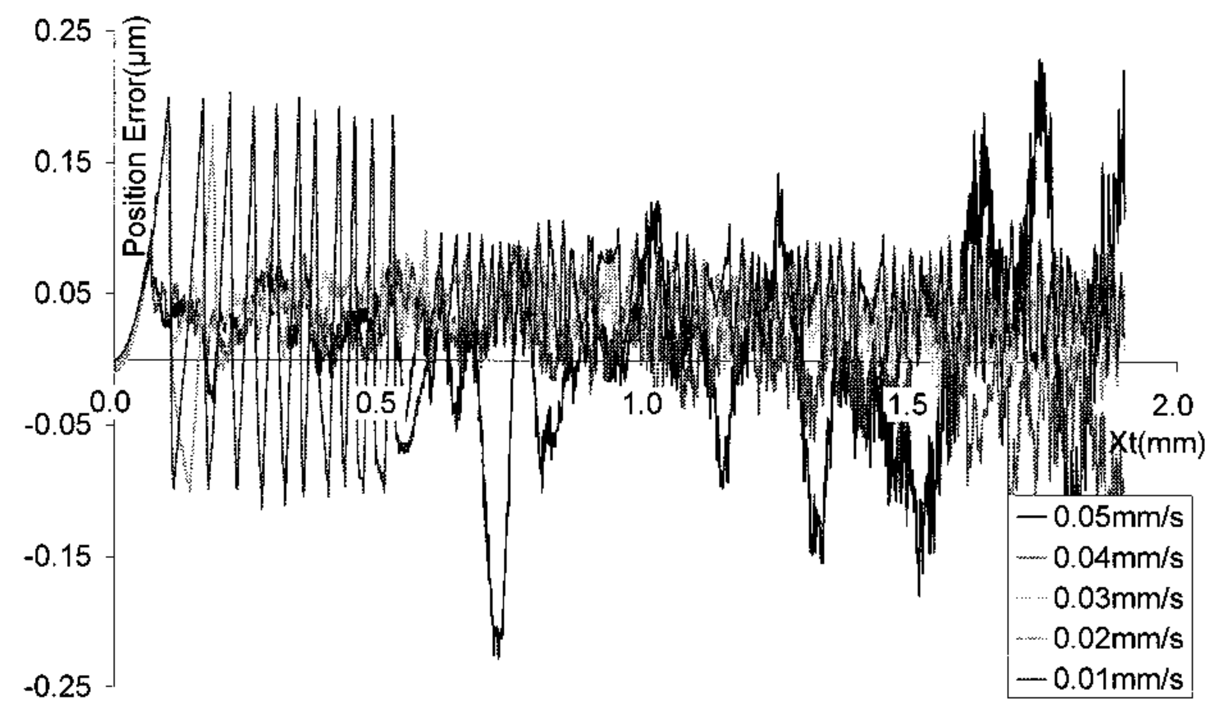

Fig. 6. Error response by feed rate variation for the convex.

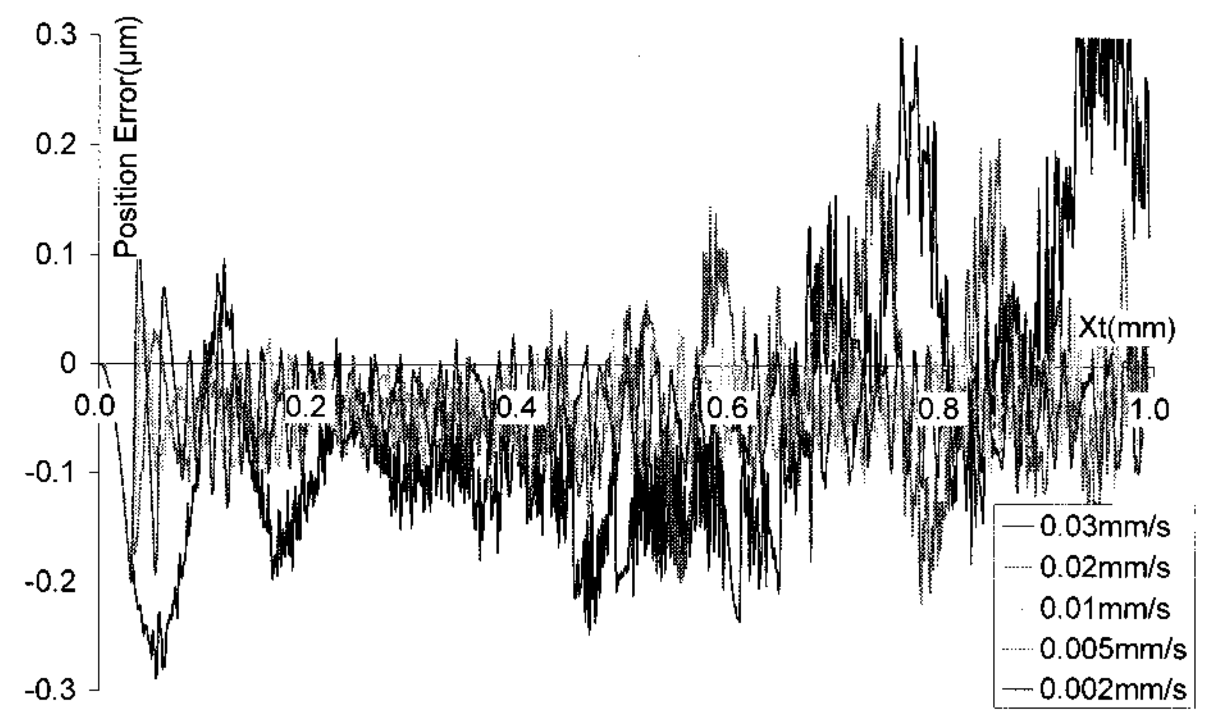

Fig. 7. Error response by feed rate variation for the concave.

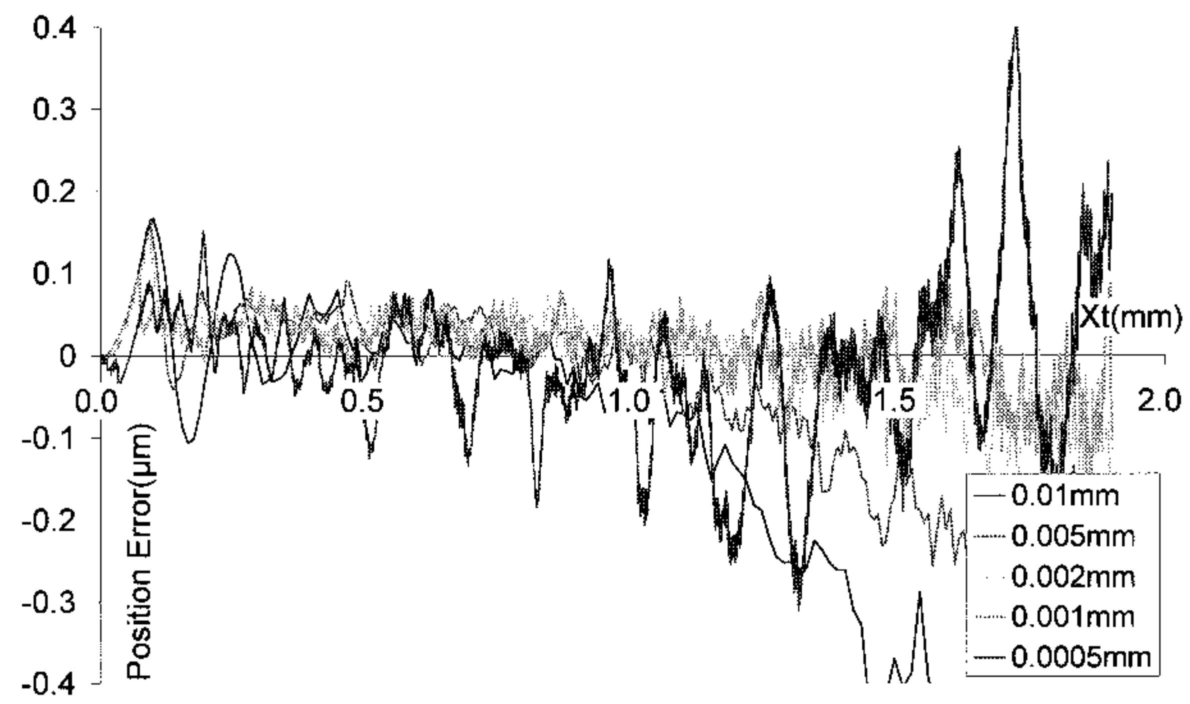

Fig. 8. Error response by control interval variation for the convex.

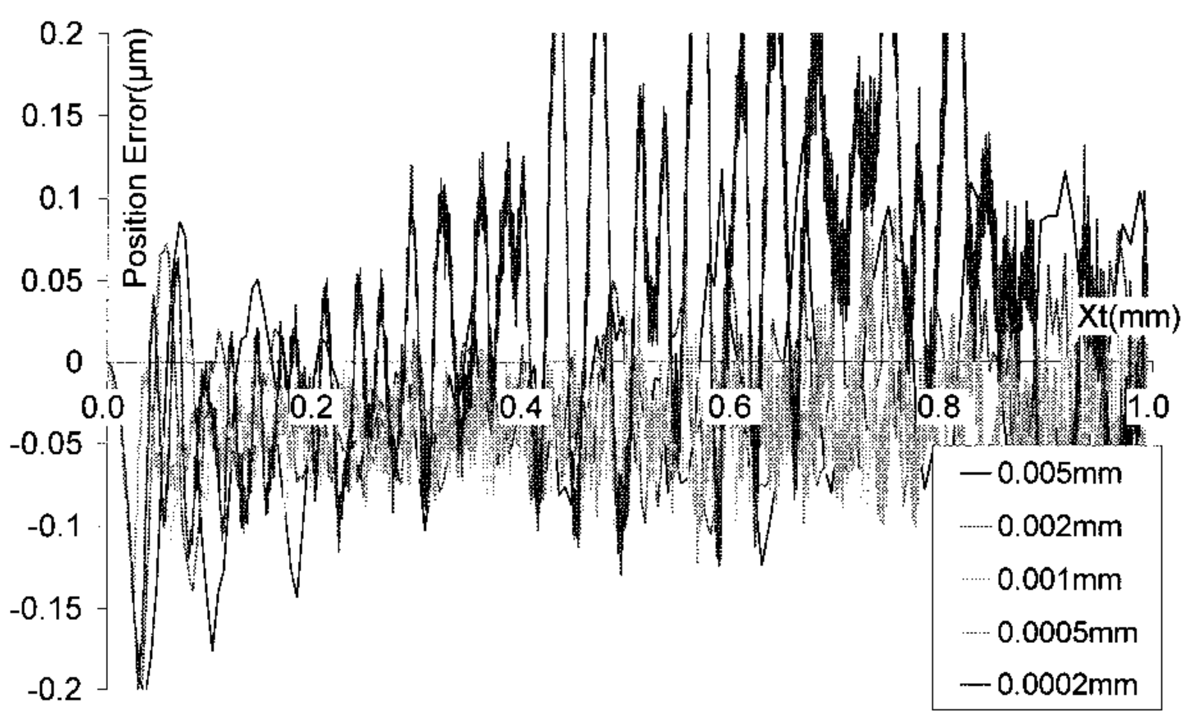

Fig. 9. Error response by control interval variation for the concave.

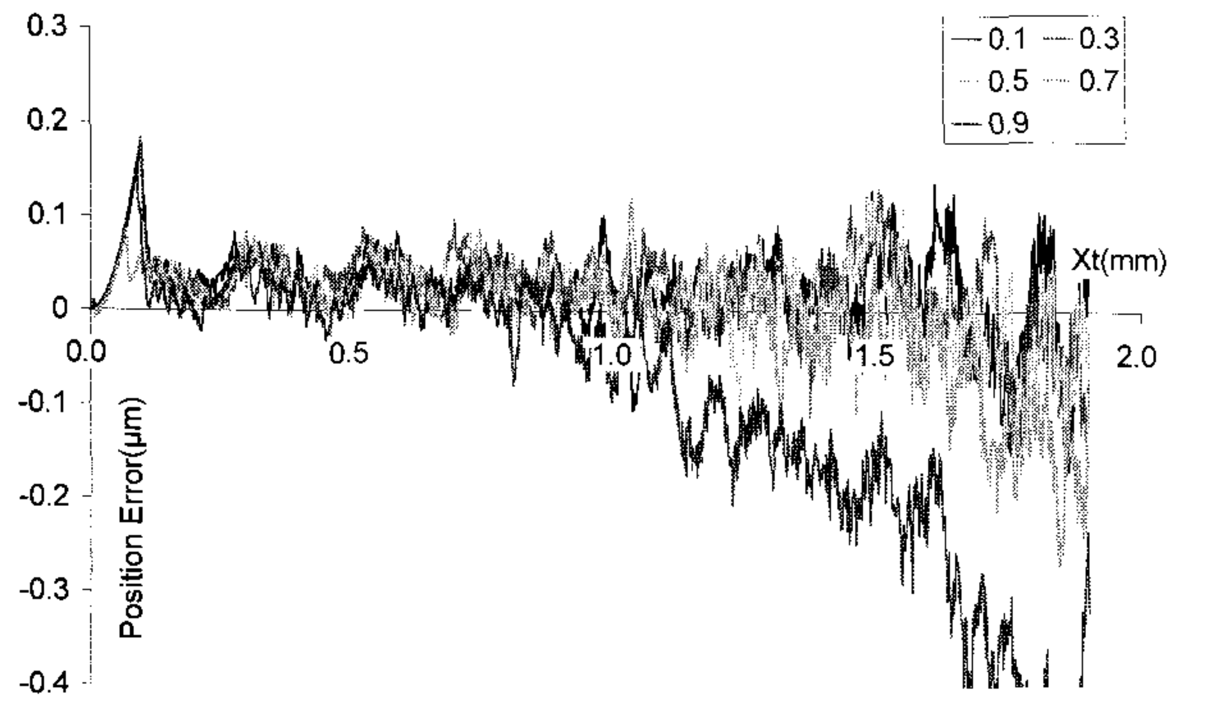

Fig. 10. Error response by smoothness variation for the convex.

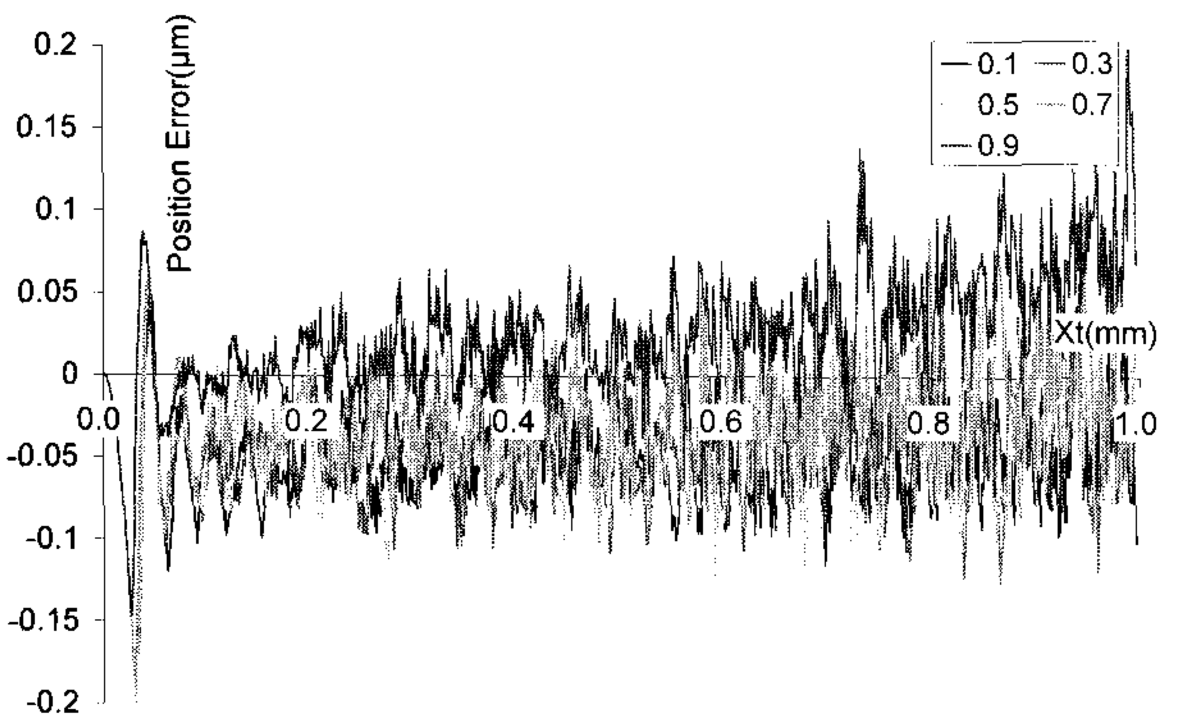

Fig. 11. Error response by smoothness variation for the concave.

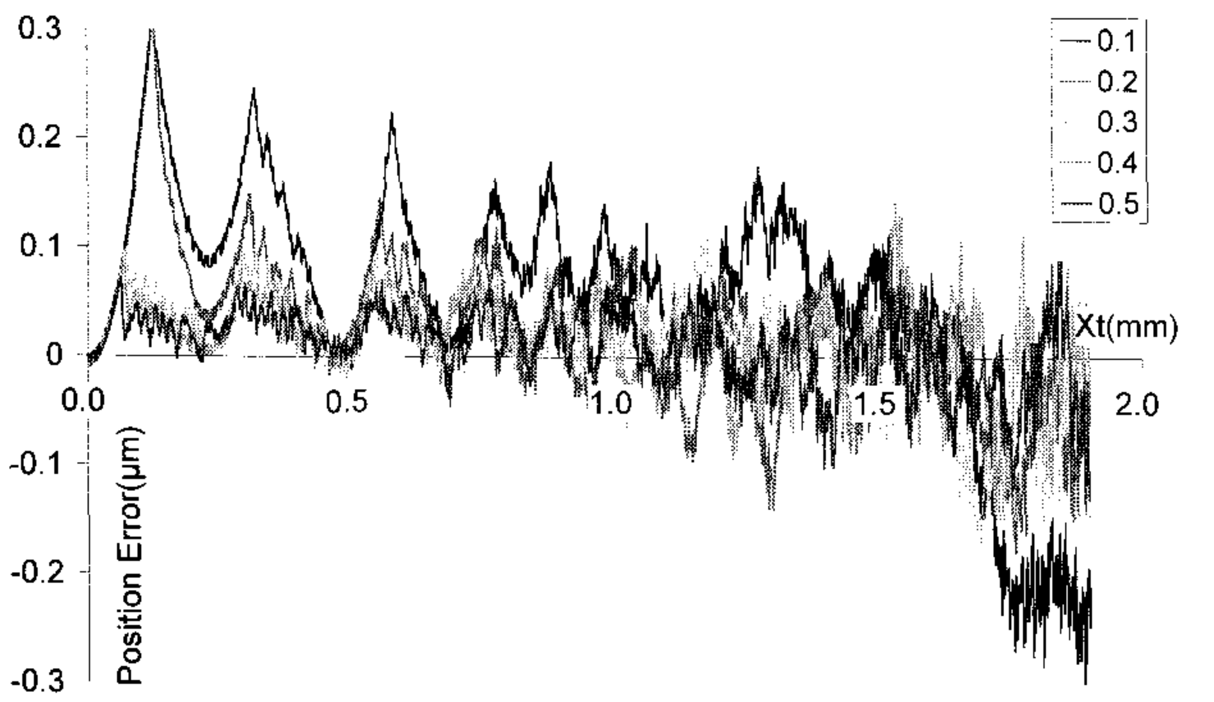

Fig. 12. Error response by position gain variation for the convex.

The initial peak can be reduced by higher gain and the saw-teeth curves also decreased. But this parameter affects to control stability, so the higher gain can make the system unstable. The error increased by the x stroke, which is similar to above results. The response of K_p is shown at Figs. 12 and 13.

The response of the velocity gain is shown as Figs. 14 and 15. The trend between K_v and the error was not clear on the convex surface, but the initial peak decreased by higher gain. The error around the circumference of a lens increased with higher gain on the convex.

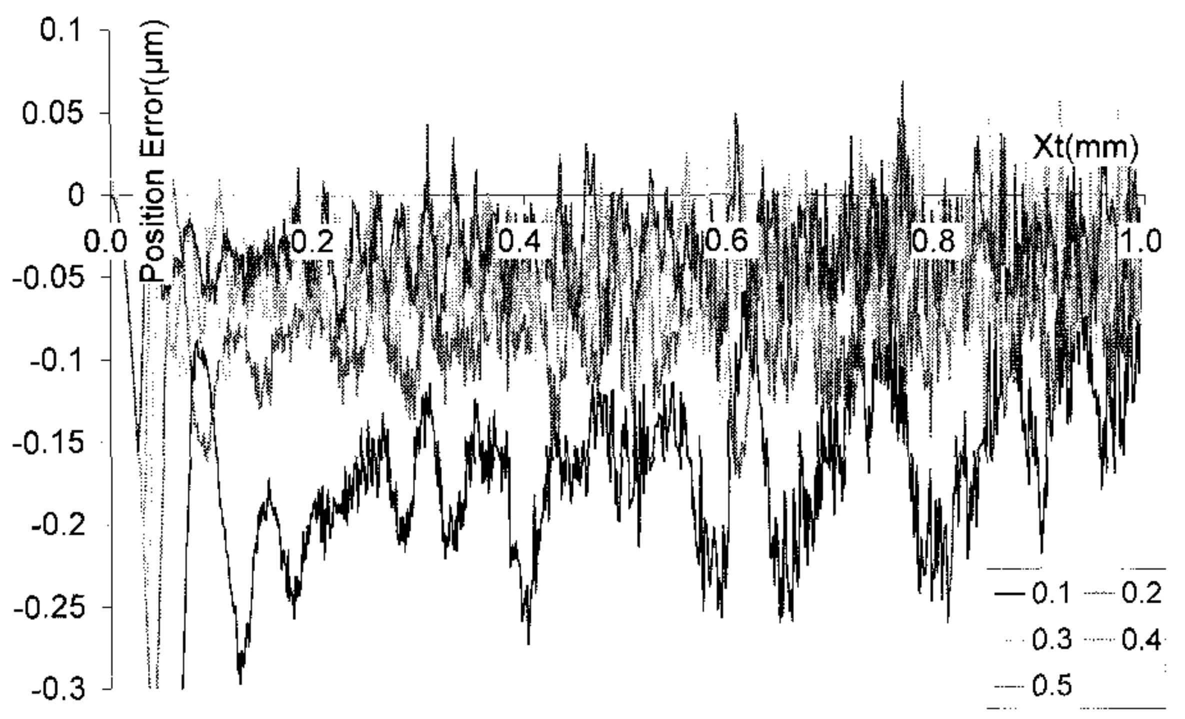

Fig. 13. Error response by position gain variation for the concave.

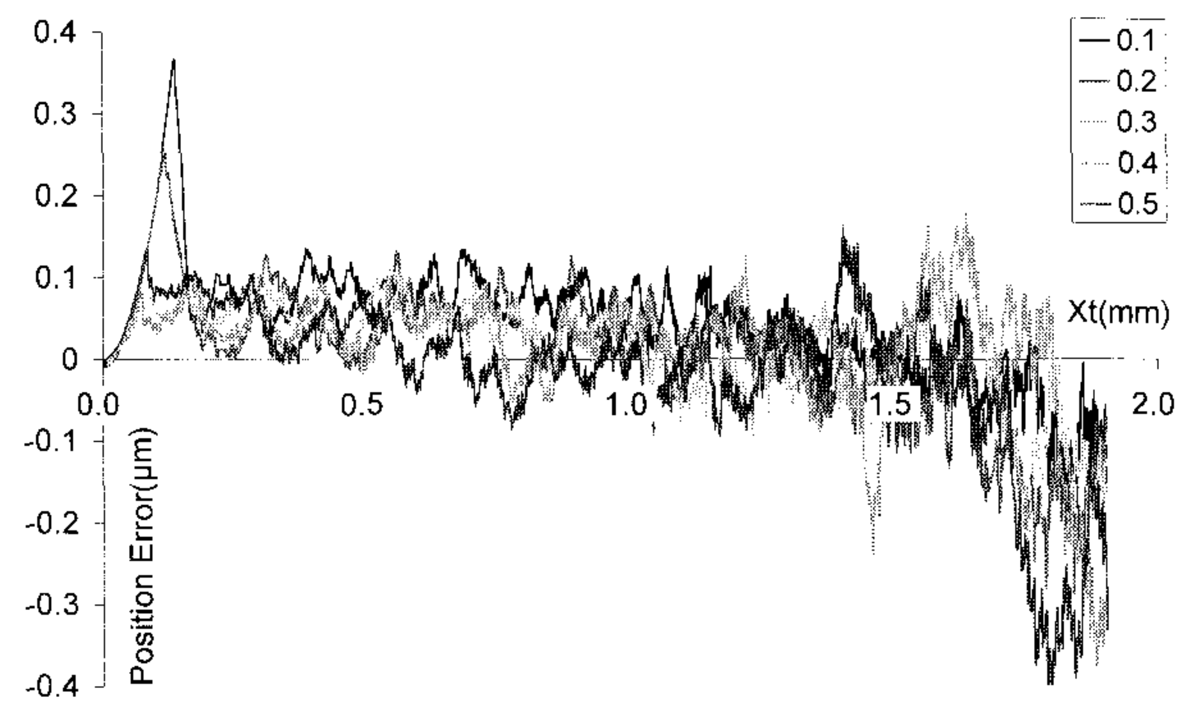

Fig. 14. Error response by velocity gain variation for the convex.

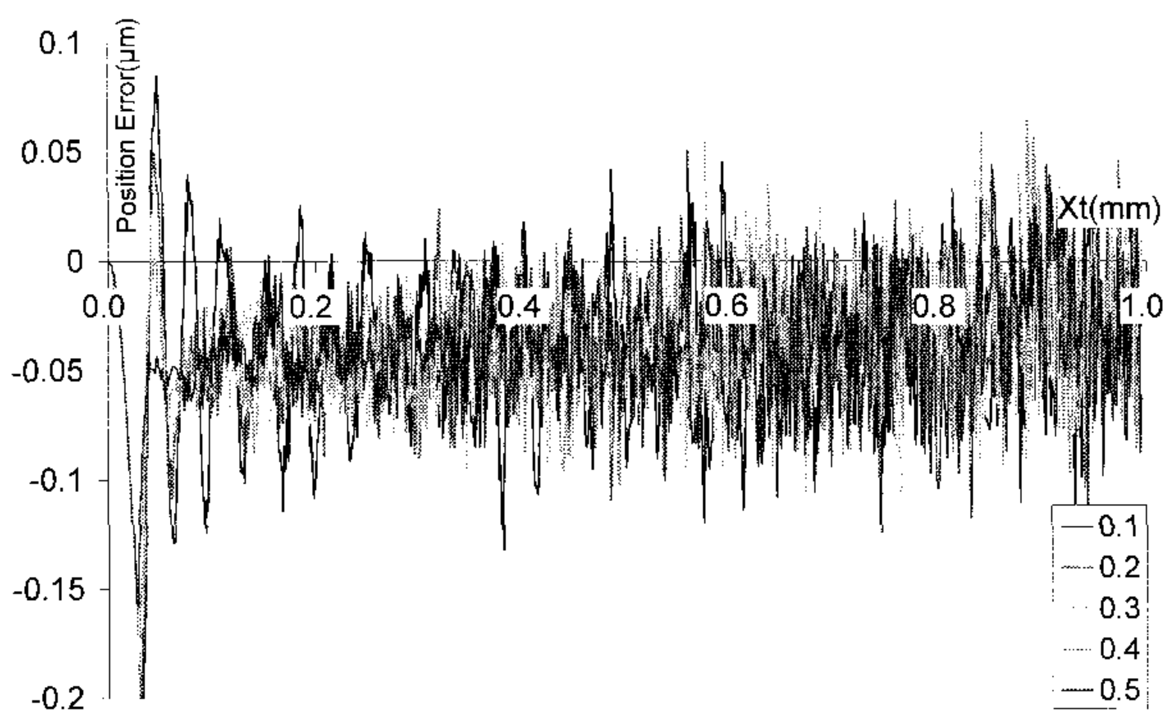

Fig. 15. Error response by velocity gain variation for the concave.

The initial position error can be reduced a little by the increment of K_v. In the experiment, we found that this factor diminished the oscillation of the error response, so the value should be determined in the suitable range.

From the effect of each parameters, optimized parameters were determined and applied to the experiment system. The parameters for the convex lens were $\delta = 0.0005$, $\delta = 0.5$, $v_f = 0.01$mm/s, $K_p = 0.4$ and $K_v = 0.2$. Those of the concave lens were $\delta = 0.0002$, $v_f = 0.002$mm/s and others are equal to the convex.

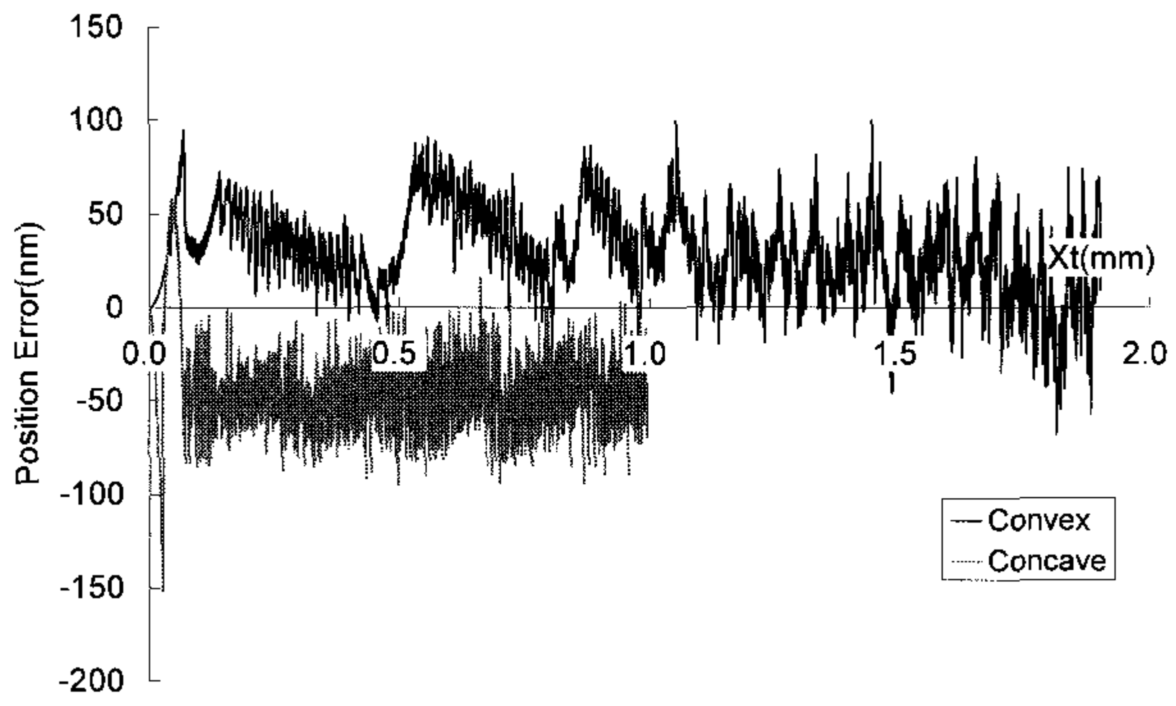

Fig. 16. Error response by optimized parameters.

The result in Fig. 16 shows that the maximum error of the convex surface was below 100nm, and that of the concave was below 150nm. There was an initial peak at each graph, but the error was varied around the average line.

6. CONCLUSIONS

Control algorithm for tool path for grinding and polishing aspheric surface was reviewed. The curve of tool path was partitioned by an interval. The ideal velocity and accelerations were calculated by feed rate, size of interval and smoothness at each section. The actual velocity during processing was determined from the ideal values, position error and control gains. The time base equations were converted to position base ones. In the experiment, nano resolution system was constructed and controlled by the proposed algorithm. The control parameters were varied and position error was monitored.

From the response of the parameter variation, optimized parameters were obtained. The best result from the values showed that the maximum error of the convex surface was below 100nm and that of the concave was below 150nm. The author found that this velocity base algorithm has enough performance for grinding and polishing aspheric lens.

REFERENCES

[1] M. Sekine, N. Sugimoto, and H. Wakatsuk, "Press-formed aspherical micro lense made of Bismuth based glass with high refractive index and transparency," *Proc. of Optical Fiber Communication Conf.*, vol. 1, pp. 91-106, 2004.

[2] W. C. Chen and F. G. Tseng, "Tunable micro-aspherical lense manipulated by 2D electoro static force," *Proc. of Int. Conf. on Solid-state Sensors, Actuators and Microsystems*, pp. 376-379, 2005.

[3] L. Zhang, T. S. Kuriyagawa, T. Y. Kaku, and J. Zhao, "Investigation into electrorheological fluid-assisted polishing," *International Journal of Machine Tools & Manufacture*, vol. 45, no. 12-13, pp. 1461-1467, May 2005.

[4] Y. C. Lee, C. M. Chen, and C. Y. Wu, "A new excimer laser micromachining method for axially symmetric 3D microstructures with continuous surface profiles," *Sensors and Actuators A (physical)*, vol. 117, no. 12-13, pp. 117-355, 2005.

[5] V. C. Venkatesh, S. Izman, S. Sharif, T. Y. Mon, and M. Konneh, "Precision micro-machining of silicon and glass," *Proc. of IEEE Int. Conf. on Industrial Application and Technology*, pp. 1146-1151, 2002.

[6] C. Y. Jhuang, J. Y. Chen, and T. D. Cheng, "A design of scanning system based on aspherical lens," *Proc. of the Second Asia and Pacific Rim Symp. on Biophotonics*, pp. 148-149, 2004.

[7] A. Y. Dyomin, S. M. Marchuk, and V. I. Reizlin, "Simulating a non-spherical surface profile," *Proc. of the 9th Russian-Korean Int. Symp. on Science and Technology*, pp. 592-593, 2005.

[8] M. Y. Yang and H. C. Lee, "Local material removal mechanism considering curvature effect in the polishing process of the small aspherical lens die," *Journal of Material Processing Technology*, vol. 116, no. 2-3, pp. 298-304, 2001.

[9] H. T. Kim and H. J. Yang, "Semi-continuous interpolation algorithm for aspherical surface grinding," *Proc. of IEEE Region 10 Conf.*, pp. 1-5, 2005.

[10] H. T. Kim, H. J. Yang, and S. C. Kim, "A study on the control method for the tool path of asherical surface grinding and polishing," *Journal of the Korean Society of Precision Engineering*, vol. 23, no. 1, pp. 113-119, 2006.

[11] R. R. Shannon, *The Art and Science of Optical Design*, Cambridge, United Kingdom, 1997.

[12] W. Tai, R. Schwarte, and H. G. Heinol, "Optimisation of the light transmission and irradiance distribution of an aspherical lens for 3-D time-of-flight sensors," *Optics & Laser Technology*, vol. 32, no. 2, pp. 111-116, 2000.

[13] M. Hill, M. Jung, and J. W. MacBride, "Separation of form from orientation in 3D measurements of aspheric surfaces with no datum," *International Journal of Machine Tools & Manufacture*, vol. 42, no. 4, pp. 456-466, 2002.

[14] H. T. Kim, H. J. Yang, and S. C. Kim, "Nano control algorithm for grinding and polishing aspherical surface," *Proc. of the IEEE Conf. Emerging Technologies and Factory Automation*, pp. 113-119, 2006.

[15] E. S. Lee and S. Y. Baek, "A study on optimum grinding factors for aspheric convex surface microlens using design of experiments," *International Journal of Machine Tools & Manufacture*, vol. 47, no. 3-4, pp. 509-520, 2007.

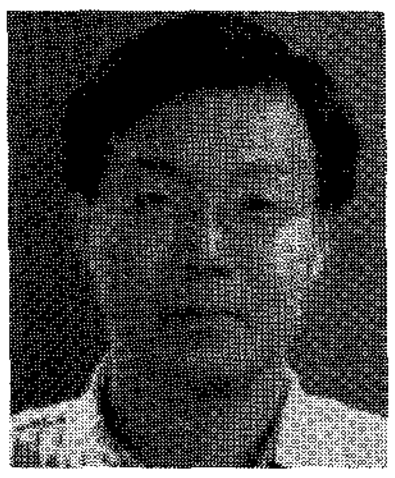

Hyung-Tae Kim received the Ph.D. degree in Precision Mechanical Engineering from Hanyang University in 2005. He is currently a Researcher in the Mechatronics Team of Korea Institute of Industrial Technology. He has written 15 papers in the international journals and conferences. He is a Reviewer in the SCI journals and the IEEE conferences. His research interests include control algorithms, automation methods, semiconductor manufacturing machines, vision-motion systems, and industrial programs.

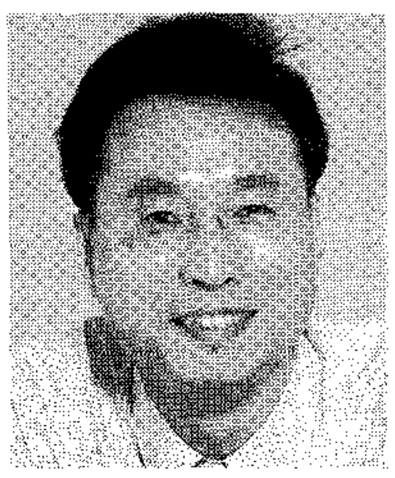

Hae-Jeong Yang received the Ph.D. degree in Precision Mechanical Engineering from Hanyang University in 1997. He is currently a Professor in the Mechanical Design Engineering of Korea Poly-technique University. He has published more than 20 papers in the journals and conferences. He reviews the papers of the domestic journals. His research interests include the design of automatic machines, machine tool design, hydraulic-pneumatic systems and CAD/CAM.

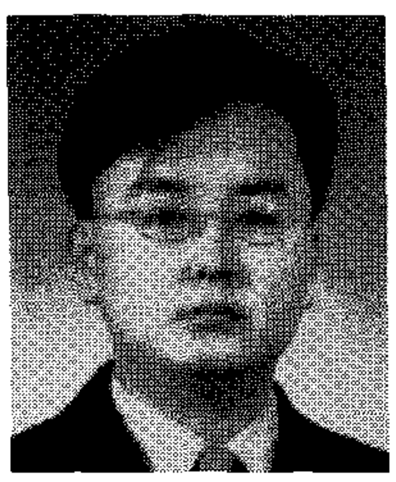

Sung-Chul Kim received the M.S. degree in Precision Mechanical Engineering from Busan National University in 2000. He is currently a Deputy Manager in the research center of AM Technology. He accomplished 4 national projects and is carrying out a grinding machine. He has published 5 papers and holds 5 patents. His research interests include grinding and polishing of ceramic material.